

## Reverse color sequence in the diffraction of white light by the wing of the male butterfly *Pierella luna* (Nymphalidae: Satyrinae)

Jean Pol Vigneron,<sup>1,\*</sup> Priscilla Simonis,<sup>1</sup> Annette Aiello,<sup>2</sup> Annick Bay,<sup>1</sup> Donald M. Windsor,<sup>2</sup>  
Jean-François Colomer,<sup>1</sup> and Marie Rassart<sup>1</sup>

<sup>1</sup>Research Center in Physics of Matter and Radiation (PMR), University of Namur (FUNDP), 61 rue de Bruxelles,  
B-5000 Namur, Belgium

<sup>2</sup>Smithsonian Tropical Research Institute, Apartado 0843-03092 Balboa, Ancón Panamá, Republic of Panama  
(Received 26 December 2009; revised manuscript received 29 May 2010; published 4 August 2010)

The butterfly *Pierella luna* (Nymphalidae) shows an intriguing rainbow iridescence effect: the forewings of the male, when illuminated along the axis from the body to the wing tip, decompose a white light beam as a diffraction grating would do. Violet light, however, emerges along a grazing angle, near the wing surface, while the other colors, from blue to red, exit respectively at angles progressively closer to the direction perpendicular to the wing plane. This sequence is the reverse of the usual decomposition of light by a grating with a periodicity parallel to the wing surface. It is shown that this effect is produced by a macroscopic deformation of the entire scale, which curls in such a way that it forms a “vertical” grating, perpendicular to the wing surface, and functions in transmission instead of reflection.

DOI: [10.1103/PhysRevE.82.021903](https://doi.org/10.1103/PhysRevE.82.021903)

PACS number(s): 42.66.-p, 42.70.Qs, 42.81.Qb

### I. INTRODUCTION

*Pierella luna* (Fabricius, 1793) is a very common butterfly from Central America. It belongs to the large family Nymphalidae, and is classified as a member of the subfamily Satyrinae. The often used English vernacular name for this butterfly, “forest-floor satyr,” is suggested by the male’s habit of resting on the ground, where he is protected by his cryptic color, with the wings held together over the back (Fig. 1). The brown color of this butterfly indeed closely matches the various browns of the plant debris and soil of the tropical forest floor. Males appropriate themselves in flat, open, yet still shady, areas, such as a section of a forest trail, which they may share with one or two other males, and which they patrol in search of females. The females move freely about the forest and are not confined to trails, so that their encounters with males are rather exceptional. The biology of these butterflies, and, in particular, the sensitivity of their populations to the persistence of the tropical dry season has been investigated by Aiello [1] on populations found on Barro Colorado Island, in the Republic of Panama.

One characteristic of the male, not found in the female, is the iridescence of the forewings. This reflection, which changes dramatically in hue depending upon the angle of view, is shown in the lower photograph in Fig. 2. When the upper (dorsal) side of the wing is viewed under white light, it flashes color that, at the angle shown in the photograph, appears green. The beam of light in this case, was set to approximately 45° of incidence, as measured from the direction perpendicular to the wing plane (the “vertical” direction). The color produced by the wing structure changes over a wide range of the human visible spectrum depending on the viewing direction. Viewed with the naked eye, violet is formed at a grazing emergence angle and as this angle is changed, the various rainbow colors are viewed in sequence,

from blue through orange. Red should also be seen, but its intensity is so low that it is difficult to distinguish from the brown pigmented background of the wing.

Rainbow coloration by diffraction of light by a grating has been reported previously for a butterfly [2]: the cross-ribs of the scales of *Lamprolenis nitida* (Nymphalidae), a New-Guinean forest butterfly, also belonging to the Satyrinae, diffract light to produce a range of colors from red to green, backscattered in the forward direction, under anteroposterior illumination. In that case, the color response can be associated with the order  $m=-1$  produced by a wing-scale diffraction grating lying nearly flat along the wing surface. However, the sequence of the colors differs from that observed in *Pierella luna*. In *Lamprolenis*, with a grating step of the order of 580 nm, a white beam directed roughly along the normal direction generates a red diffracted beam at grazing emergence. In that case, the other colors, orange, yellow,



FIG. 1. (Color online) The male butterfly *Pierella luna*, subject of the present study, at rest on the ground. ©Steve Collins, reproduced with permission.

\*[jean-pol.vigneron@fundp.ac.be](mailto:jean-pol.vigneron@fundp.ac.be)

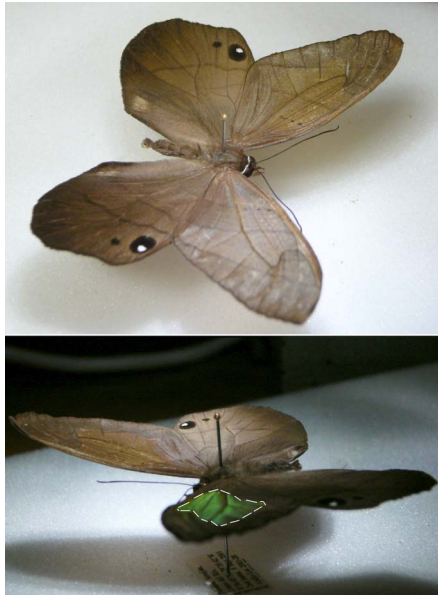


FIG. 2. (Color online) The male butterfly *Pierella luna* shows, under most illumination angles, an inconspicuous brown color that closely matches the colors of the forest floor. However, under very specific illumination and viewing angles, rainbow iridescence appears in the central portion of the forewing, the area inside the dashed line in the lower view.

green, appear at smaller angles, increasingly closer to the vertical direction. Thus, grazing red starts the color sequence in *Lamprolenis nitida*, as in all similar butterflies that have a diffraction grating lying flat on the wing surface.

As shown in Fig. 3, in *Pierella luna*, the sequence of the colors is reversed, compared to *Lamprolenis*. The blue end of the spectrum exits under a grazing angle, while the red end emerges closer to the direction perpendicular to the wing. If we think of a structure built on a flat scale, it is difficult to imagine a specific ultrastructure that would produce an “inverted” diffraction. As is often the case, the natural device—as we will see later—reveals a disarmingly simple solution to this problem.

Such coloration, found in the male but not in the female, most likely is an intraspecific signal that facilitates courtship and/or identifies males as males, and not females to be courted [3,4]. A comparative behavioral study of *Lamprolenis nitida* and *Pierella luna* might explain how these direct and inverted patterns can affect the biology of these butterflies but, to our knowledge, such investigations are still to be undertaken. Before providing a microscopic view of the structure and a model to explain how the reverse color sequence is produced, we will present a more quantitative characterization of the optical properties of the dorsal wing surface in *Pierella luna*.

## II. OPTICAL PROPERTIES

An Avaspec 2048/2 fiber-optic spectrophotometer was used to assess the optical properties of the wing. The measurement chain was equipped with a combined equilibrated halogen-deuterium source covering 250–1100 nm, slightly

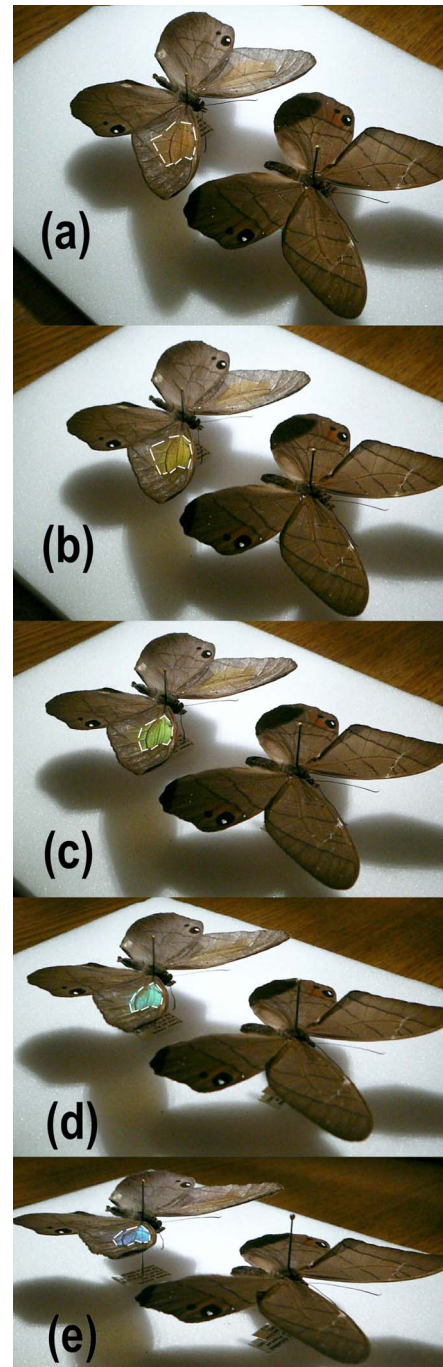


FIG. 3. (Color online) Male and female *Pierella luna* butterflies viewed at different angles. The male is behind the female. The illumination is  $45^\circ$  from the normal, and originates from a point opposite to the viewer. As we lower our angle of view with a fixed light source, the delineated area on the forewing of the male butterfly displays a rainbow of iridescence, covering nearly the entire human spectrum: in positions (a), (b), (c), (d), and (e), red, yellow, green, cyan, and blue are perceived, respectively. The female lacks iridescence.

exceeding the human visible spectral range. In these measurements, the intensity is systematically compared to the intensity scattered from a standard, diffusive white, polytetrafluoroethylene reference surface (Avaspec), under identical

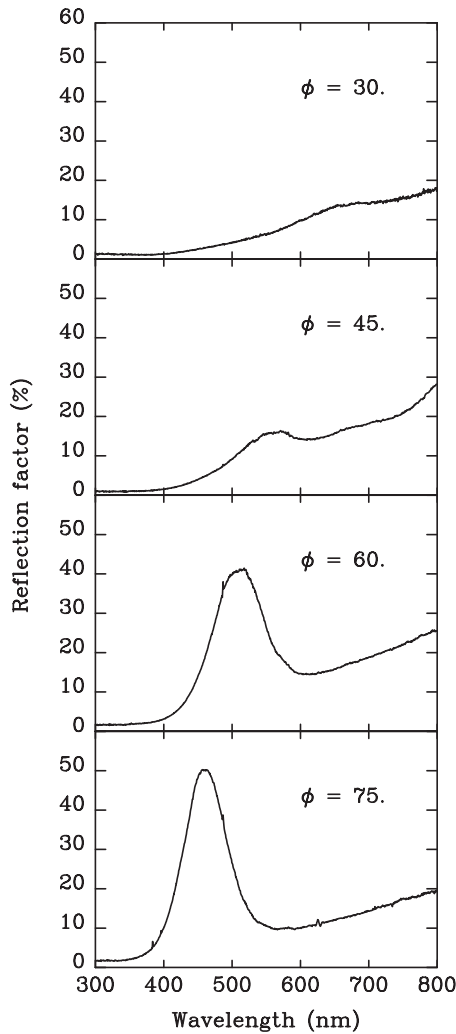


FIG. 4. Spectral distribution of the light measured from the iridescent portion of the wing of the male butterfly *Pierella luna* at various viewing angles  $\phi$  (emergence angle measured from the vertical). The illumination source (oriented toward the wing tip at  $45^\circ$ ) and the probe are opposite with regard to the vertical, in the measurement plane.

configurations. With this normalization, the reflected intensity usually is referred to as a “reflection factor,” expressed in %. This quantity is not bound to be less than 100%.

For the present study, we worked with the subspecies *Pierella luna luna*, collected in the Republic of Panama, near Panama City, and on Barro Colorado Island [5]. We also used the subspecies *Pierella luna heracles*, collected in Mexico. Several males and one female belonging to the latter subspecies were studied. No difference in optical properties could be noticed between both subspecies.

The reflection factor of the dorsal side of the forewing, under various angles of emergence, is shown in Fig. 4. The measurement plane crosses the wing from base to apex. The illumination is oriented toward the wing apex and the collecting probe receives the light that is scattered forward. The light beam makes an angle  $\theta=45^\circ$  with the vertical (incidence angle) and the probe collects light exiting from the

wing under various emergence angles  $\phi$ , also measured from the “vertical.” This illumination direction is only an average efficient direction to produce colored reflection: the same effect can be perceived over a wide ( $\pm 30^\circ$ ) range of angles about this direction. However, the effect is partly destroyed if the incident light is diffuse, as iridescence then desaturates the color produced.

As Fig. 4 shows, the perceived color of the scattered light changes with the emergence angle. All the spectra reveal a single band (the “iridescent signal,” of structural origin), which overlays a reddish brown background (the pigmented coloration of the wing, visible from most view points). Close to the vertical emergence ( $\phi=30^\circ$ ), the iridescence is very broad and weak, and is centered on the dominant wavelength  $\lambda=650$  nm, a wavelength already classified as “red” [6] in the chromaticity diagram [7]. The intensity of the iridescence increases and wavelengths shift to shorter as viewing angle increases, i.e., moves away from the vertical. At the emergence  $\phi=45^\circ$ , the iridescent band is somewhat better defined, with a dominant wavelength of 570 nm, in the human “greenish yellow” region. When  $\phi$  reaches  $60^\circ$ , the iridescent band shifts to  $\lambda=500$  nm, located at the frontier of the “bluish green” zone. Finally, for  $\phi=75^\circ$ , close to a grazing angle, the iridescent band is much stronger and is centered on  $\lambda=460$  nm, which corresponds to “purplish blue,” as seen by humans.

In order to explain these coloration properties, the most common structural mechanisms—a flat grating or a flat multilayer—can both be ruled out. For a light beam of wavelength  $\lambda$  incident at an angle  $\theta$ , the grating with period  $b$  generates diffracted beams of various spectral orders exiting at different emergence angles  $\phi$ , given by

$$\sin \phi = \sin \theta + m \frac{\lambda}{b}, \quad (1)$$

$m$  is an integer labeling the diffraction order. The deviation from specularity in orders different from zero is stronger for long wavelengths  $\lambda$  than for short wavelengths. In other words, in a flat scale grating system, the blue color emerging from white light decomposition is always less diffracted. In *Pierella luna* iridescence, the blue exits under an angle more distant from specularity than does light of longer wavelengths, such as orange. In other words, there is no way for a flat grating model to fit the observed sequence of colors that emerge from the decomposition of white light by *Pierella luna*. As well, an explanation based on the color change produced by a multilayer structure would require a correlated change between the incidence angle and the emergence angle, an effect not seen in *Pierella luna*.

The visual effect produced by *Pierella luna* then cannot be described by either a grating or a multilayer parallel to the wing surface. In the next section, we will investigate the structure of the wing and the structures inside the scales in order to provide an explanation for this surprising, likely new, visual effect.

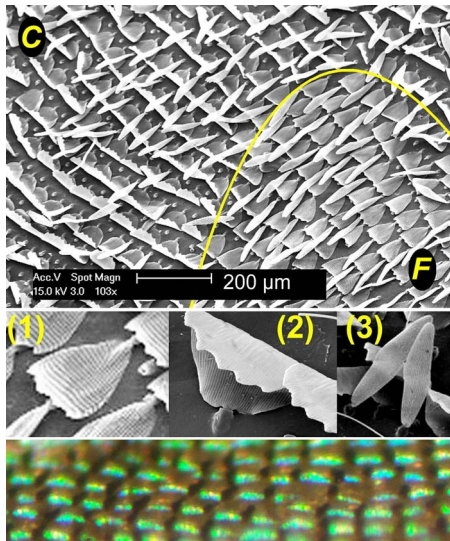


FIG. 5. (Color online) This figure shows the three types of scales found on the dorsal surface of male *Pierella luna* forewings. Type (1) (see insert) lies flat against the wing membrane in the normal, noniridescent portion of the wing; type (2) found in the iridescent portion of the wing is curled, with the distal end protruding high above the wing surface; type (3) is a narrow tube, also protruding high above the wing surface. The zone occupied by curled scales (c) is sharply delineated (as indicated by the solid line) from that occupied by flat scales (f). Those parts of the wings that are not iridescent (including the ventral sides) bear resemblance to the (f) areas. On the lower part of the figure, a light-microscope grazing angle view shows that the iridescence originates from the curled scales of type (2). The tubular scales-type (3)-appear dark.

### III. NANOMORPHOLOGY

For this investigation, small areas of a male *Pierella luna* wing were selected at the border of the iridescent zone. They were cut and attached, dorsal surface up, to a sample holder using carbon tape, then metal coated (20 nm of gold), and examined with two scanning electron microscopes (SEM). A low-resolution Philips XL20 was chosen for preliminary explorations and a JEOL 7500F high-resolution field-emission SEM was used for more detailed examinations.

A low-resolution picture of the male forewing surface, showing the arrangement of the scales, is seen in Fig. 5. Three types of scales are visible on this picture: (1) straight scales, lying flat against the wing membrane, are seen only in the area denoted as “F” (=flat); (2) longitudinally curled scales, protruding high above the wing surface are distributed only in the area denoted as “C” (=curled); (3) narrow, transversely curved, tubular scales, can be seen in both zones, arranged between the other two types of scales. On most butterflies, two layers of scales can be distinguished: the ground scales, which form the lower layer, close to the wing membrane, and the cover scales, covering the ground scales. The tubular scales here, in the male, could be interpreted as cover scales but this classification is not very relevant here.

In the female, the ground scales and the cover scales are similar, but the former appear white, while the latter are brown. Only scales of type (1) are apparent (no curled

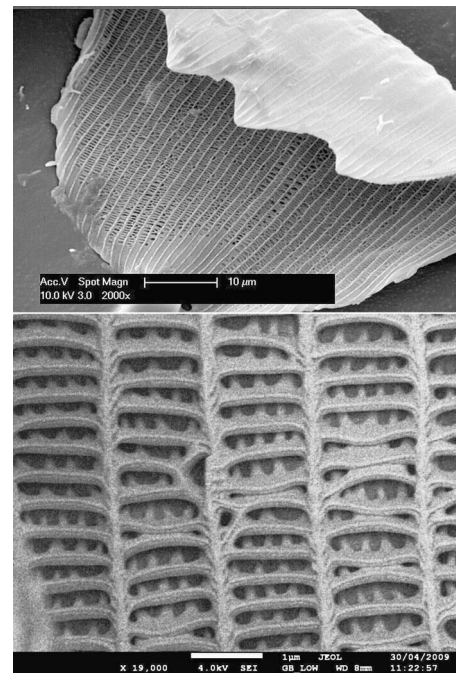


FIG. 6. Scanning electron microscope image of a curled scale of a male *Pierella luna*, showing its structure. The ribs (vertical structures shown in the lower portion of the figure) and the cross-ribs (horizontal) are attached directly to the scale basal membrane. We note the absence of any other structure (often referred to as a “pepper-pot”) between the net of ribs and cross-ribs and the basal membrane. The distance between the cross-ribs is small, on the average, 440 nm (corrected for a perspective effect on the SEM picture

scales), and no iridescence is ever produced. That finding is consistent with the observation that, on the male, the iridescent zone corresponds to area “C,” made up of curled and tubular scales. The narrow, transversally curled, scales (type 3) appear dark under an optical microscope at all illumination angles, suggesting that the origin of the male iridescence should be searched for on the curled scales (type 2). That idea is confirmed by light-microscope pictures, such as that in the lower portion of Fig. 5, which shows the blue–green color of the tips of the curled scales, under an appropriate illumination and viewing angle.

The ultrastructure of a curled (type 2) scale is shown in Fig. 6. Lepidopteran scales are large, flattened cells, and thus have two cell wall layers, dorsal and ventral. In the figure, we see the apical portion of the scale’s ventral surface, which consists of a homogeneous, continuous, membrane with no significant structure. We see also, the basal portion of the scale’s dorsal surface which appears to be perforated, and can be described as a longitudinal array of parallel “ribs,” separated by a distance of 1.5  $\mu\text{m}$ . These ribs are connected by “cross ribs,” regularly spaced along the length of the scale, and separated by a much shorter distance,  $b = 440$  nm, on average. The cross rib distances fluctuate somewhat, but mostly locally, when a defect modifies the shape of an isolated cross rib. This general uniformity permits the array to function as a diffraction grating. The cross ribs have evolved a lamellar shape, each lamella being con-

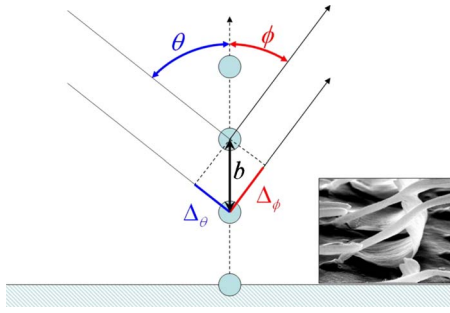


FIG. 7. (Color online) Configuration of an upright grating that functions in transmission. The angle of incidence  $\theta$  is measured from the vertical to the basal plane, i. e. from the grating plane. The angle of emergence  $\phi$  is measured from the same direction. The picture shows a lateral view of the transversely curled scales (type 2) that alternate with the narrow, longitudinally curled scales (type 3).

nected to the lower face membrane by, on average, 3 or 4 thin trabeculae. This structure is much like that encountered in the butterfly *Lamprolenis nitida*, already mentioned, in which the grating is found on scales that lie flat against the wing. In *Pierella luna*, the height of the flattened cross-ribs is however much shorter than in those of the New-Guinean butterfly. The use of this grating is also completely different here, because the portion of the scale responsible for the color effect is actually upright, and perpendicular to the wing surface. Furthermore, in *Pierella luna* the grating is used in transmission instead of in reflection. We could not find any other report of such a use of a grating for animal coloration.

In the next section, we develop a simple model to explain the color sequence in an upright grating, used in transmission. The function of the tubular scales (type 3) is intriguing. Their narrow shape leave space for the type 2 scales to curl up. However, they also appear with an identical shape between flat scales. Their original function may well be related to completely different engineering purpose, such as providing hydrophobicity or ease the flow of air on the wing surface during flight.

#### IV. VERTICAL GRATING USED IN TRANSMISSION

Understanding how an upright grating decomposes a white light beam is rather elementary. The geometry is sketched in Fig. 7. A grating with period  $b$  is set upright, oriented vertical to the basal plane, which, in our case, is the plane of the butterfly wing. The incident light beam is set at an angle  $\theta$  to the vertical.  $\theta$  is then measured from the grating plane. We consider the light emerging at an angle  $\phi$ , also measured from the vertical to the basal plane. The difference in the paths of the two rays scattered by two successive cross ribs is the sum

$$\Delta_{\theta} + \Delta_{\phi} = b \cos \theta + b \cos \phi. \quad (2)$$

A constructive interference will build up when the path difference matches an integer multiple of the light wavelength  $\lambda$ . This interference leads to the relationship between the incident wavelength and the emergence angle

$$\cos \phi = -\cos \theta + m \frac{\lambda}{b}. \quad (3)$$

If we consider the grating step  $b=440$  nm measured on a *Pierella luna* wing scale, this model provides far-field solutions for only the orders  $m=0$  and  $m=1$ . For all other integers (including  $m=-1$ ), the emergence angle  $\phi$  comes out as a complex number, which means that the diffracted wave is evanescent and is not observed.  $m=0$  is the immediate “specular” case, for which the direction is independent of the incident wavelength. It gives the solutions

$$\phi = \pi - \theta \quad (4)$$

and

$$\phi = \theta - \pi. \quad (5)$$

The first solution is simply a light ray transmitted as a continuation of the incident light beam, which keeps a straight path and is directed toward the wing membrane. This emerging ray is absorbed or diffused and cannot produce iridescence. The second solution is the incident beam specularly reflected (not transmitted) by the grating. That ray also is lost in the wing membrane and cannot contribute to the iridescence.

With  $\theta=45^{\circ}$ , the iridescence actually comes from the solutions for  $m=1$ . In that case, the emergence angle  $\phi$  depends on the incident light wavelength  $\lambda$  (the color of the incident light), so that, in that diffraction order, decomposition of white light occurs. If we consider a long-wavelength “yellowish green” light at 550 nm, we get the solutions

$$\lambda = 550 \text{ nm}: \phi = 57.1^{\circ} \quad (6)$$

and

$$\lambda = 550 \text{ nm}: \phi = -57.1^{\circ}. \quad (7)$$

The first solution is the “transmitted” diffraction order, while the second is the “reflected” one. For a shorter wavelength, say a blue incidence at 400 nm, we get

$$\lambda = 400 \text{ nm}: \phi = 78.3^{\circ} \quad (8)$$

and

$$\lambda = 400 \text{ nm}: \phi = -78.3^{\circ}. \quad (9)$$

Again, positive emergences correspond to transmitted rays, while negative angles describe reflected rays. The shorter the wavelength, the larger the emergence angle: blue comes out at grazing angles, and red comes out at small angles, at a near to vertical. This is the color sequence actually observed on the wing of *Pierella luna*, the inverse of what is observed on a “horizontal” grating, such as that developed by *Lamprolenis nitida*.

Quantitatively, however, the agreement between the calculated and observed emergence angles is not perfect, though the model of a vertical grating correctly predicts the color sequence. As seen in the insert of Fig. 7, the grating is not exactly vertical: it is actually slanted in the direction of the butterfly body, toward the light source, and it is slightly curved, not flat. Only the apical part of the scale contributes to the coloration, as revealed by the optical microscope im-

TABLE I. Angle of emergence from a grating slanted in the direction of the source, assuming a grating slant angle of  $20^\circ$ . The grating periodicity is  $b=440$  nm. The angles of emergence are given for each of the dominant frequencies found in the experimental spectra in Fig. 4.  $\phi_{exp}$  is the emergence angle set in the experimental geometry.  $\phi_{calc}$  is calculated from the formula (10) for the given wavelength

$\lambda$ (nm)	$\phi_{exp}$	$\phi_{calc}$
650	$30^\circ$	$35^\circ$
570	$45^\circ$	$47^\circ$
500	$60^\circ$	$57^\circ$
460	$75^\circ$	$62^\circ$

age in Fig. 5. The slant angle can be estimated by fitting the observed emergence angles:  $\gamma=20^\circ$ . Though this slant angle varies widely for different scales, this value is representative of the observed scales tip geometry. The formula (3) should be slightly modified to adjust for this slant angle:

$$\cos(\phi + \gamma) = -\cos(\theta - \gamma) + m \frac{\lambda}{b} \quad (10)$$

where, as before, the angles  $\theta$  and  $\phi$  are measured from the vertical, which now does not coincide precisely with the orientation of the grating.

The results are given in Table I, which lists the emergence angles, obtained from the spectral measurements in Fig. 7 ( $\phi_{exp}$ ) and from the use of formula (10) ( $\phi_{calc}$ ). The trend and orders of magnitude of the emergence angles are reasonably well accounted for by the slanted transmission grating model, in spite of the irregularities of the slant angles. The variations in the values of  $\gamma$  depend on the randomly disturbed implantation of the scales on the wings, the irregularities of the grating period, which slightly varies within a given scale. The strongest approximation, however is likely to have considered a model for a planar grating, while the butterfly scale is actually curved, with a radius of curvature near  $25 \mu\text{m}$ .

More precise data on the average geometry of the scales can be extracted from measurements on a much larger number of upright scales. The longitudinal profile of an average scale is shown in the insert of Fig. 8. The individual scatterers, distant of  $440$  nm, empirically follow a curve defined as

$$x = b \left\{ 1 - \left( \frac{z-a}{a} \right)^{2n} \right\} \quad (z \leq a)$$

$$x = b + (c-b) \left( \frac{z-a}{d-a} \right)^{2m} \quad (z \geq a). \quad (11)$$

The coordinate  $x$  measures the grating scatterer position from the pedicel, along the length of the scale, while  $z$  measures its height above the membrane. A realistic shape of the scale is obtained with  $m=n=1$ . The average geometric parameters are given by  $a=21.4 \mu\text{m}$ ,  $b=57.9 \mu\text{m}$ ,  $c=45.6 \mu\text{m}$ , and  $d=50.65 \mu\text{m}$ , and the grating is simulated by 41 longitudi-

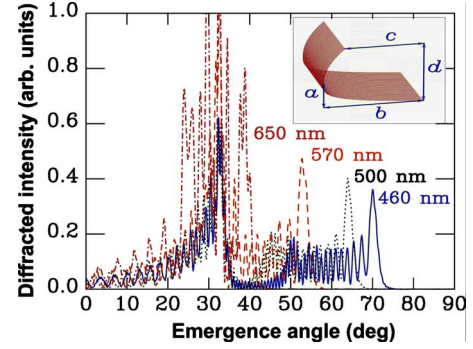


FIG. 8. (Color online) Angular distribution of the light intensity emergent from a collection of about 10 000 pointlike scatterers disposed on a surface following an average scale shape (as shown in the insert). The distance between the scatterers, in the rows along the curved direction, is  $440$  nm, while the distance between rows, in the perpendicular direction is  $1.3 \mu\text{m}$ . The angular distribution of intensities is obtained as the interference of all waves emitted by the scatterers, in the first Born approximation. From the geometric point of view, this model is more realistic than the “vertical” planar grating model from Fig. 7. It also predicts a reverse ordering of the color emergences and better explains the angular range spanned by the diffracted beams.

nal rows of point scatterers, separated, laterally, by a distance of  $1.3 \mu\text{m}$ . The Fraunhofer diffraction of an incident plane wave by this curved grating has been calculated, in the first Born approximation and for isotropic scattering, as a function of the emergence direction, for different wavelengths. In this approximation, it is known [8] that the diffracted amplitude  $A(\vec{k}')$  in the direction indicated by the wavevector  $\vec{k}'$  is the Fourier transform of the scattering strength distribution function. For a collection of  $N$  identical scatterers distributed at locations  $\vec{r}_\ell$  in space ( $\ell=1,2,\dots,N$ ), the diffracted intensity will be proportional to

$$|A(\vec{k}')|^2 \propto \left| \sum_{\ell=1}^N e^{i(\vec{k}'-\vec{k})\cdot\vec{r}_\ell} \right|^2, \quad (12)$$

where  $\vec{k}$  is the incident wavevector, here oriented at  $45^\circ$  from the perpendicular to the wing plane and  $\vec{k}'$  is the emergent wave vector, measured from the same reference. For the simulation reported here, the light is assumed to be directed along the curvature of the scale surface. The wavelength  $\lambda$  of the incident radiation is related to the light wave vector and is conserved, as with all elastic scattering processes:

$$|\vec{k}'| = |\vec{k}| = \frac{2\pi}{\lambda}. \quad (13)$$

The Fraunhofer diffraction is shown in Fig. 8, for four wavelength values in the visible range, as a function of the emergence angle  $\phi'$ , measuring the distance between the emerging wave vector  $\vec{k}'$  and the vertical axis. For each wavelength, contrasting the case of the better known planar grating, the intensity is spread on a broader range of outgoing directions, but there is, in each case, a preferred emergence angle, clearly indicated by a peak, on the large angle

side of the diffracted band. The blue scattering is predicted under  $70^\circ$  ( $75^\circ$ , experimentally) and the red contribution ranges about  $30^\circ$ , as indeed observed, confirming the reverse ordering of colors explained by a vertical grating structure. The contribution near  $30^\circ$  of emergence is, however, complicated by contributions from the reflection (zero-order diffraction) of other colors from the near-horizontal part of the scale. This greatly desaturates the red color: indeed, this color is difficult to distinguish from the pigmentary brown background in experimental spectra (Fig. 4).

We also considered, using the same approach, the propagation of light first reflected by the wing membrane. For an incidence originating from under the scale, it is found that very little diffraction occurs, so that most of the light is transmitted along a straight path, with no color dependence. This suggests that the reflection on the membrane only contributes to the brown background color.

It should be emphasized that the models developed in this section are based on point-like scatterers and, because of this, are not suited to describe the *intensity* of the observed spectra. The change of spectral intensity for different angles in Fig. 4 can however be understood in terms of the blaze given to the grating by the actual lamellar shape of the cross ribs, which constitute the grating scatterers. In a grating, a flat profile, slanted in the direction of the forward illumination will favor diffraction at large angles, which match the reflection condition on the scatterer surface. In the present case, red diffraction, which comes under smaller angles, are less intense.

In principle, a vertical grating can be illuminated from both sides and decomposes light in both direction: it is indeed easy to observe also white light decomposition when the forewing is illuminated from the tip apex. In this case, however, the incident light should be set to a more grazing direction. Under some fixed diffuse illumination—as that expected in a narrow open area in the forest—this multiple light scattering process may deliver quite a complex signal, in particular when the butterfly is flapping the wings in flight.

## V. CONCLUSION

The wings of male *Pierella luna* butterflies display a distinctive type of iridescence produced by the decomposition of white light by redirecting visible colors into specific emergence angles. Compared to many other Nymphalidae species that decompose white light using a diffraction grating, this particular butterfly is special in that the sequence of the colors is reversed. Our investigation of this butterfly demon-

strates that this inversion results from the use of a grating to transmit rather than reflect the components of the decomposed light beam, a feat achieved by the unusual configuration of some of the wing scales, which are curved in such a way that the grating is “vertical,” mounted perpendicular to the wing surface.

The biological significance of the optical effect described in the present paper, and in particular the impact of the color order reversal, is still far from elucidated. The fact that only males show the multiscale structure that leads to the colored signal, and not females, indicates that the purpose is intraspecific. It could be useful for courtship or, between males, for territory control. Many field experiments are still needed to assess the most plausible purpose of the specific visual effect. For example, it would be important to determine the visual capabilities of the male and the female, and study the courtship relative motions in order to determine the importance of the visual effect in the mating success. It would be important as well to determine the male capacity to use the signals to organize the territory occupation. Or discover other, more subtle, possible functions. All this requires long observations in the field or more experimentation.

The fabrication of an artificial version of such a specialized grating might be regarded as a formidable task when considered from the point of view of micro-engineering. In fact, the structure of a butterfly’s wing surface, with its covering of flat, structured scales, requires only a minimal modification to produce the “Pierella effect:” it is simply enough that the scales curl up, without much change to the ultrastructure. Indeed, the modification occurs on a scale much larger than the structures responsible for the light interferences. The radius of curvature of the scales is of the order of  $25\ \mu\text{m}$ , which stresses the importance of multiscale descriptions of natural photonic devices [9]. Modifications to the geometry on a scale much larger than the wavelength of light can have dramatic consequences for the way the structural coloration device works.

## ACKNOWLEDGMENTS

The authors thank Steve Collins for the permission to reproduce the picture in Fig. 1. Namur Interuniversity Scientific Computing Facility (Namur-ISCF) was used for computations. M.R. and J.-F.C. were supported by the Belgian National Fund for Scientific Research (F.R.S.-FNRS). J.P.V. and M.R. acknowledge the hospitality of the Smithsonian Tropical Research Institute (STRI), in the Republic of Panama, during the earliest stages of this work.

- 
- [1] A. Aiello, in *Insects of Panama and Mesoamerica: Selected Studies*, edited by D. Quintero and A. Aiello (Oxford University Press, New York, 1992), pp. 573–575.  
 [2] A. L. Ingram, V. Lousse, A. R. Parker, and J. P. Vigneron, *J. R. Soc., Interface* **5**, 1387 (2008).  
 [3] R. Silberglied, in *The Biology of Butterflies*, edited by R. I.

Vane-Wright and P. R. Ackery (Academic Press, New York, 1984), pp. 207–410.

- [4] C. Wiklund, in *Butterflies: Ecology and Evolution Taking Flight*, edited by C. L. Boggs, W. B. Watt, and P. R. Ehrlich (The University of Chicago Press, Chicago, 2003), pp. 67–90.  
 [5] E. I. Huntington, *Bull. Am. Mus. Nat. Hist.* **63** (3), 191 (1932).

- [6] K. L. Kelly, *COLOR Universal Language and Dictionary of Names* (U.S. Department of Commerce, U.S.A., 1976).
- [7] *Commission Internationale de l'Eclairage Proceedings, 1931* (Cambridge University Press, Cambridge, England, 1932).
- [8] N. W. Ashcroft and N. D. Mermin, *Solid State Physics* (Harcourt Brace College, Fort Worth, 1976).
- [9] J. P. Vigneron, M. Ouedraogo, J.-F. Colomer, and M. Rassart, [Phys. Rev. E \*\*79\*\*, 021907 \(2009\)](#).